AGU PUBLICATIONS

JGR

Journal of Geophysical Research: Atmospheres

RESEARCH ARTICLE
10.1002/2017JD026697

Key Points:
- Cold surges from extratropical South America can influence lower tropospheric circulation over subtropical North Atlantic in June–August
- An anomalous cross-equatorial shallow circulation induced by the low-tropospheric temperature gradient is responsible for such an influence
- Weak upper tropospheric westerlies over the southern Amazon are required to allow deep penetration of the cold surges into the Amazon

Correspondence to:
R. Fu,
rfu@atmos.ucla.edu

Citation:
Bowerman, A. R., R. Fu, L. Yin, D. N. Fernando, P. A. Arias, and R. E. Dickinson (2017), An influence of extreme southern hemisphere cold surges on the North Atlantic Subtropical High through a shallow atmospheric circulation, *J. Geophys. Res. Atmos.*, *122*, 10,135–10,148, doi:10.1002/2017JD026697.

Received 21 FEB 2017
Accepted 9 JUL 2017
Accepted article online 21 JUL 2017
Published online 5 OCT 2017

©2017. American Geophysical Union. All Rights Reserved.

An influence of extreme southern hemisphere cold surges on the North Atlantic Subtropical High through a shallow atmospheric circulation

A. R. Bowerman[1], R. Fu[2], L. Yin[1], D. N. Fernando[3], P. A. Arias[4], and R. E. Dickinson[1]

[1]Departmental of Geological Sciences, University of Texas at Austin, Austin, Texas, USA, [2]Department of Atmospheric and Oceanic Sciences, University of California, Los Angeles, California, USA, [3]Texas Water Development Board, Austin, Texas, USA, [4]Grupo de Ingeniería y4 Gestión Ambiental, Escuela Ambiental, Universidad de Antioquia, Medellín, Colombia

Abstract Previous studies have attributed interhemisphere influences of the atmosphere to the latitudinal propagation of planetary waves crossing the equator, to the triggering of equatorial Kelvin waves, or to monsoonal circulation. Over the American-Atlantic sector, such cross-equatorial influences rarely occur during boreal summer due to unfavorable atmospheric conditions. We have observed that an alternative mechanism provides an interhemisphere influence. When episodes of extreme cold surges and upper tropospheric westerly winds occur concurrently over southern hemisphere Amazonia, cold surges from extratropical South America can penetrate deep into southern Amazonia. Although they do not appear to influence upper tropospheric circulation of the northern hemisphere, extremely strong southerly cross-equatorial advection ($>2\sigma$ standard deviations, or 2) of cold and dense air in the lower troposphere can reach as least 10°N. Such cold advection increases the northward cross-equatorial pressure gradient in the lower to middle troposphere, thus shallow northerly return flow below 500 hPa. This return flow and the strong lower tropospheric southerly cross-equatorial flow form an anomalous shallow meridional circulation spanning from southern Amazonia to the subtropical North Atlantic, with increased geopotential height anomalies exceeding $+1\sigma$ to at least 18°N. It projects onto the southern edge of the North Atlantic Subtropical High (NASH), increasing its pressure and leading to equatorward expansion of NASH's southern boundary. These anomalies enhance the NASH, leading to its equatorward expansion. These extreme cold surges can potentially improving the predictability of weather patterns of the tropical and subtropical Atlantic, including the variability of the NASH's southern edge.

1. Introduction

Teleconnection between the Northern and Southern Hemisphere contribute to dynamic disturbances in tropical regions, such as those of Asia-Australia and the eastern Pacific-South America. For example, *Radok and Grant* [1957] found a connection between the upper level westerly wind in the Australian sector and that of the northern hemisphere during boreal winter (December–February). *Lau and Li* [1984] suggested that cold surges, referred to as strong cold fronts of extratropical origin, from Eurasia can influence convection over the tropical central Pacific. *Yu and Rienecker* [1998] showed that cold surges from East Asia to the Western Pacific enhanced the magnitude of the westerly bursts that initiated the 1997–98 El Niño. *Love* [1985a, 1985b] showed that the low-level signal from Asian and Australian cold surges enhanced the low-level cyclonic shear in the opposite hemisphere and even spun up tropical cyclone activity across the equator. Over the eastern Pacific-South American sectors, *Webster and Holton* [1982] and *Tomas and Webster* [1994] have shown that planetary waves from the extratropical North Pacific can propagate to tropical eastern Pacific of the southern hemisphere and influence weather pattern there during boreal winter. *Liebmann et al.* [2009] have shown that the planetary waves from the northern hemisphere tropical eastern Pacific can excite convective-coupled equatorial Kelvin waves over South America that propagate eastward and influence rainfall and zonal winds over the equatorial Atlantic and Africa [*Wang and Fu*, 2007].

The mechanisms behind the teleconnection between the northern and southern hemispheres reported in literature include cross-equatorial planetary wave propagation; extratropical forced equatorial Kelvin waves [*Hoskins and Yang*, 2000; *Liebmann et al.*, 2009; *Straub and Kiladis*, 2002], the low-level cross-equatorial flow associated with deep monsoonal circulation [*Lau and Li*, 1984; *Wang and Fu*, 2002; *Fu et al.*, 2016], or shallow meridional circulations [*Zhang et al.*, 2008]. Latitudinal planetary wave propagation requires

westerlies in the upper troposphere [*Charney*, 1963, 1969; *Dickinson*, 1970]. Such upper tropospheric westerlies are referred to as the "westerly duct," in which the waves of zonal scales less than the zonal scale of the westerly duct may propagate from one hemisphere to the other [*Webster and Holton*, 1982]. Such a westerly duct commonly occurs in the eastern Pacific and the Atlantic [*Tomas and Webster*, 1994] during boreal winter where upper tropospheric (200 hPa) westerlies prevail. During boreal summer (June–August), these regions are dominated climatologically by upper tropospheric easterlies at the equator (5°S–5°N), leading to the absence of such a westerly duct so preventing cross-equatorial propagation of planetary waves.

Over the South America, cold air incursions occur year around. They are especially strong and can penetrate deeply into southern Amazonia in the austral winter/dry season or boreal summer [*Parmenter*, 1976; *Marengo et al.*, 1997; *Garreaud and Wallace*, 1998; *Vera and Vigliarolo*, 2000; *Lupo et al.*, 2001; *Pezza and Ambrizzi*, 2005; *Li and Fu*, 2006; *Liebmann et al.*, 2009]. However, these cold surges generally cannot reach equatorial areas (5°S–5°N) [*Garreaud*, 2000]. The dry atmosphere at this time of year also prevents these cold surges from producing large-scale increases of deep convection in southern Amazonia. Thus, they rarely trigger convectively coupled equatorial Kelvin waves in the South America-Atlantic sector during boreal summer [*Liebmann et al.*, 2009]. Low-level cross-equatorial flow may also allow one hemisphere to influence the circulation of the other hemisphere. For example, the cross-equatorial flow over the western Amazon has a strong influence on the Amazonian rainfall distribution on seasonal, intraseasonal, and interannual scales [*Wang and Fu*, 2002]. It has been suggested that the onset of the monsoon over South America may contribute to an abrupt demise of the North America monsoon through the reversal of the cross-equatorial flow [*Fu et al.*, 2016]. However, such an interhemisphere connection appears to be part of the deep monsoonal circulation driven by deep convection in the summer hemisphere, and it is limited to the tropical region. Whether cold surges in winter of the southern hemisphere can affect atmospheric circulation in the summer of the northern hemisphere beyond the tropics has not been reported in literature for the American-Atlantic sector or elsewhere.

This study aims to explore the mechanisms that provides north-south hemisphere teleconnections in the atmosphere induced by the deeply penetrating equatorward incursions of cold surges from extratropical South America during boreal summer (austral winter), when the previously identified mechanisms involving anomalous deep tropospheric circulation for interhemisphere connection are inactive. To clarify the link of such potential interhemisphere influence, we evaluate its impact on the North Atlantic Subtropical High (NASH), i.e., the "Bermuda High," which has been shown in literature to affect summer weather patterns over the eastern and central United States [*Davis et al.*, 1997; *Diem*, 2006; *Li et al.*, 2011].

The NASH is a semipermanent feature of the low-level atmospheric circulation over the North Atlantic [*Davis et al.*, 1997; *Diem*, 2006]. Its climatological core is anchored over the central and eastern North Atlantic, but it exhibits substantial variability in both intensity and morphology at daily, interannual, and decadal time scales [*Davis et al.*, 1997; *Diem*, 2006; *Li et al.*, 2011]. The variability of the NASH, particularly the boreal summer expansion of its western ridge into the western North Atlantic and the Gulf of Mexico, has profound impacts on the circulation over the Intra-Americas [*Henderson and Vega*, 1996], including the low-level moisture transport into North America [*Li et al.*, 2011, 2013], and the timing of the demise of the North American monsoon [*Arias et al.*, 2012]. The westward expansion of the NASH can trigger severe midsummer droughts across the Intra-Americas [*Kelly and Mapes*, 2011], leading to an early demise of the North American monsoon and late onset of the South American monsoon over southern Amazonia [*Arias et al.*, 2015], and may influence the routing of North Atlantic tropical cyclones [*Wang and Lee*, 2007].

Many competing hypotheses have been proposed regarding the mechanisms that control the variability of the NASH. Some authors have suggested that the subtropical anticyclones over the Pacific and Atlantic Oceans arise from zonally asymmetrical subtropical heating patterns forced by the Asian monsoon [*Chen et al.*, 2001; *Rodwell and Hoskins*, 2001]. Alternatively, many studies have emphasized the importance of heating contrasts between the land and adjacent oceans for the NASH. For example, *Seager et al.* [2003] have suggested that differential diabatic heating and atmospheric interactions with ocean currents must be important for the strengthening of the NASH to its observed magnitude. *Liu et al.* [2004] have suggested that monsoonal heating and dynamically induced descent are not necessary for the formation of the subtropical anticyclones, but that they can instead be initiated by column diabatic heating contrasts between continent

and ocean. Furthermore, it has been suggested that surface heating contrasts between the Atlantic and North America continents dominate the climatology and variability of the NASH [*Miyasaka and Nakamura*, 2005; *Li et al.*, 2011, 2012]. Most of the studies of the NASH's variability have focused on the east-west variation of its ridge. Few papers have studied the causes of the meridional variability of its southern ridge. Among them, *Li et al.* [2012] have attributed the equatorward migration to a strengthening of the NASH core. Whether other factors can influence the meridional variation of the NASH has not been reported in literature.

This study explores whether cold surges from extratropical South American can impact circulation of the northern hemisphere tropics and subtropics, especially the southern flank of the NASH. If so, what processes could contribute to such an influence in the absence of a prevailing westerly duct over equatorial South America and the tropical North Atlantic. The data and methods are detailed in section 2, and the results and figures are described in section 3. Discussion of the mechanism, its broader implications, and main sources of uncertainty are given in section 4. Conclusions are provided in section 5.

2. Data and Methods

In this study, we use the Modern-Era Retrospective Analysis for Research and Applications (MERRA) product [*Rienecker et al.*, 2011], provided by the Global Modeling and Assimilation Office. This reanalysis product is averaged into daily fields on a global 1.25° latitude × 1.25° longitude grid over the time period from 1979 to 2013, with data spanning the tropospheric column (1000 hPa to 100 hPa) at specified pressure levels. The variables employed in this study are geopotential height, temperature, horizontal wind, and vertical velocity. The MERRA product is chosen because its daily fields appear to be less noisy than other reanalysis products, such as the European Centre for Medium-Range Weather Forecast Reanalysis-Interim (ERA-I). It is less noisy presumably because MERRA provides 3 h outputs, thus eight samples for daily means, whereas ERA-I provides 6 h outputs or four samples for daily means. The presence of convective activity associated with the leading edge of cold surges is derived from the National Oceanic and Atmospheric Administration (NOAA) Interpolated Outgoing Longwave Radiation (OLR) [*Liebmann*, 1996] data set. This data set is derived from the compilation of data from 10 NOAA satellites over the period of 1979–2013, which is then temporally and spatially interpolated onto a 2.5° latitude × 2.5° longitude global grid.

Composite analysis is used extensively in this study, with scenarios for events used for compositing selected based upon the cross-equatorial meridional wind over Amazonia (referred to as the South American monsoon V index) because of its strong correlation with geographic rainfall distribution over Amazonia [*Wang and Fu*, 2002] and the presence of upper level tropical westerlies over the same region. The V index is defined as the areal averaged 925 hPa meridional wind over 5°N–5°S, 65°W–75°W, representing the low-level cross-equatorial flow over South America. Using the V index as a basis for compositing of atmospheric variables is physically cleaner and computationally simpler than identifying South American cold surges by previously described methods [*Lupo et al.*, 2001; *Pezza and Ambrizzi*, 2005], especially when representing the influences of southern hemisphere cold surges on the northern hemisphere. In particular, we choose the events when the southerly V index is greater than its 2 standard deviations (σ) value to capture statistically significant extreme southerlies ($p < 5\%$) at the equator associated with strong cold surge events [*Garreaud and Wallace*, 1998; *Wang and Fu*, 2002]. To insure these events of extreme southerly cross-equatorial flow were caused by cold surges, we also require these events to be associated with 200 hPa zonal winds over southern hemisphere Amazonia (15°S–0°, 50°W–70°W) that are weak westerly (> 2 m s^{-1}) to ensure that the large-scale mean flow is conducive for the planetary waves associated with cold surges to propagate deep into southern tropical Amazonia [e.g., *Dickinson* 1970, *Webster and Holton*, 1982]. When easterly upper level winds occur, cold surges do not penetrate far enough into the tropics to have any impact on the northern hemisphere subtropics. When the southerly V index is greater than its 2σ value on consecutive days, only the first day is used as Day 0 for the composite. The results are not sensitive to the upper level westerly wind thresholds, as long as the threshold value is positive (westerly) within 5 m s^{-1}. Such stable results are reasonable because the westerly direction of the wind is far more important than its detailed magnitude for occurrence of the equatorward propagation of the planetary waves associated with cold surges [*Dickinson*, 1970; *Webster and Holton*, 1982]. Of the 55 events when the V index exceeds its 2σ, 30 events show the westerly 200 hPa zonal wind to be above +2 m s^{-1}. These 30 events are used for all the composite analyses in this study. We use the 200 hPa zonal

wind greater than +2 m s^{-1}, instead of 0 m s^{-1} to insure the dominance of the westerlies in the upper troposphere over our southern Amazonian domain. Only 2 out of the 55 events had 200 hPa zonal wind values that fell between ±2 m s^{-1}. If +5 m s^{-1} is used as the upper level tropical wind condition, the impact seen on the northern hemisphere is increased, but the number of composite members is reduced (not shown). This result is consistent with a stronger signal of latitudinal planetary wave propagation with an increase of the upper tropospheric westerly winds [*Tomas and Webster*, 1994].

We use the lead-lag composites to evaluate the evolution of the atmospheric circulation changes days before and after the cold surges. These lead-lag composites are made for the days before (denoted by negative number of the days), during (Day 0), and after the Day 0 conditions (denoted by positive number of the days) are met. To investigate the vertical structure of the anomalous circulation associated with the deep equatorial incursions of the southern hemisphere cold surges, we show composites of vertical and meridional wind anomalies and standardized geopotential height anomalies in the meridional-height cross-section of the troposphere ranging from 45°S to 45°N and averaged from 57.5°W to 62.5°W from 2 days before to 2 days after the cold surges.

To determine whether equatorward expansion of the NASH is significant compared to its general variability, we compare the mean June-July-August (JJA) NASH position to the composite NASH southern and western boundaries at Days −2, 0, and +1. The day −1 NASH position (not shown) is similar to that of Day −2. To determine the statistical significance of the spatial patterns, we tested its local significance by the *z*-test and verified this result by Monte Carlo simulation. We then tested their field significance using the Walker test [*Wilks*, 2006].

3. Results

The climatological distributions of the atmospheric thermodynamic and dynamic conditions during JJA over the eastern Pacific-South America-Atlantic sector are shown in Figure 1. The air temperature at 850 hPa is generally warmer over the northern hemisphere subtropics (Figure 1a), especially over the North American monsoon and Sahara, than over its southern hemisphere counterpart. The areas of deep convection, as indicated by the lowest OLR, are also centered north of the equator over the tropical eastern Pacific and the North American monsoon region, as well as over the northern hemisphere South America, Atlantic, and western Africa monsoon regions. Although the temperature is warmer over Amazonia than over the adjacent oceans, its relatively higher OLR values suggest a lack of deep convection in this region. The center of higher geopotential height and associated anticyclonic winds in the subtropical and extratropical North Atlantic (Figure 1b) mark the climatological position of the NASH. At 200 hPa, weak northeasterly winds over equatorial South America (5°S–5°N), weak easterly winds over the equatorial Atlantic (5°S–5°N), and weak westerlies over tropical South America off the equator (5°S–10°S) (Figure 1c) are evident. Such an upper level zonal wind distribution can favor the equatorward propagation of planetary waves associated with cold surges deep into tropical South America but not across the equator. In the column winds of the pressure-latitude plot (Figure 1d), the atmospheric circulation stemming from the areas of tropical convection consists of not only a deep tropospheric component but also has a shallow meridional circulation below the midtroposphere [*Nolan et al.*, 2007].

Figure 2 shows the occurrence of the deep equatorward penetrating cold surges that meet the V index and the upper tropospheric westerly thresholds described in section 2 during boreal summer for the period of 1979–2013. Such events of abnormally deep equatorward penetrations of cold surges have occurred 1–4 times or totally 1–11 days during most of the summers, more often in July and August than in June. The occurrence of these cold surge events appears to vary on interannual and decadal time scales.

The resulting lead-lag composites for the days before, during, and after the Day 0 of the selected cold surges are shown (Figure 3), with only locally significant values shown for horizontal wind and standardized temperature and geopotential height. Two days before the Day 0 (Day −2; Figures 3a and 3b) is chosen to represent the anomalous circulation pattern before the influence of cold surges near the equator. Cold surface temperature anomalies begin to form on the east side of the midlatitude Andes (Figure 3a), behind (to the southwest of) the cold fronts, as indicated by a southeastern-northwestern elongated area of anomalous low OLR. The positive geopotential height anomalies at 850 hPa (Figure 3b) have already appeared, but they are mainly confined to the southwestern Amazon and the cross-equatorial wind anomalies over South

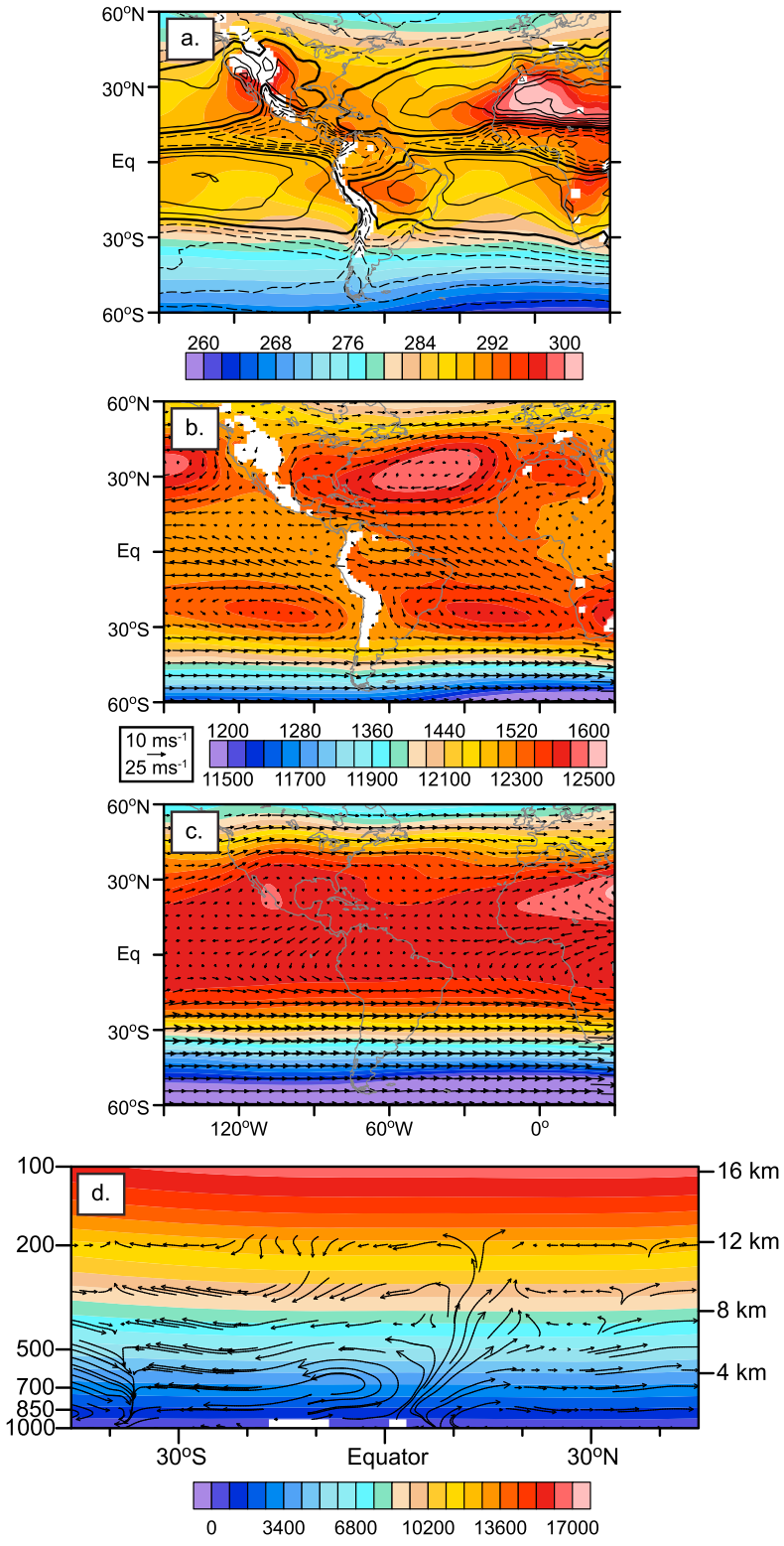

Figure 1. Summer (June–August) climatological maps for the period of 1979–2013 for (a) 850 hPa air temperature (shades) and top of atmosphere OLR (contours), where the 250 W m^{-2} contour is bolded and values above (below) 250 W m^{-2} are plotted as solid (dashed) contours at 10 W m^{-2} intervals. (b) For 850 hPa geopotential height (shading) and 850 hPa horizontal wind (vectors). (c.] Same as Figure 1b except for 200 hPa fields. (d) Summer climatological latitudinal-vertical distribution for the domain of 45°S to 45°N and 1000–100 hPa averaged over the 62.5°W to 57.5°W longitudinal sector for geopotential height (shades) and meridional circulation (vectors).

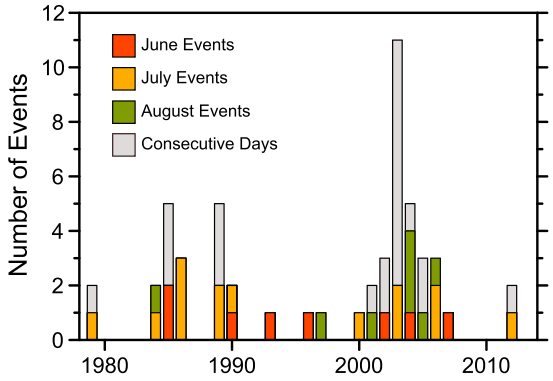

Figure 2. The number of composite events that occur in each summer month during the period of 1979 to 2013. The numbers of cold surges events occurred in June, July, and August are shown by bars in red, orange, and green, respectively. The numbers of days when the V index and the upper tropospheric westerly exceed the 2 s and +2 m s^{-1} thresholds are indicated by the total bar including in gray. They are higher than the number of cold surge events because consecutive days are considered as one cold surge event.

America are weak. The southern boundary of the NASH, shown as the bold geopotential (1560 geopotential meters (gpm)) contour, is within 1σ of the seasonal variability (Figure 4). By Day −1, the cold surface temperature anomalies enhance and expand to the southwestern Amazon (Figure 3c). The 850 hPa geopotential height also increases over nearly the entire South America and exceeds +1σ over much of the western Amazon and subtropical South America (Figure 3d). The southerly cross-equatorial low-level flow increases over South America. The NASH southwestern boundary begins to move equatorward. The increase of 850 hPa geopotential height over the equatorial Atlantic Ocean is likely a result of Kelvin waves triggered by an increase of convection, as suggested by the negative OLR anomalies over the tropical South America north of the equator (Figure 3c).

On Day 0, the day that the composite conditions described in section 2 are met, negative OLR anomalies indicate that the cold fronts move northeastward (Figure 3e). Cold surface temperature anomalies have rapidly intensified over South America and expanded into the tropical North Atlantic (Figure 3e). Higher geopotential anomalies at 850 hPa (Figure 3f) have increased to greater than +1σ across the entire South American continent and into the subtropics of the northern hemisphere, with geopotential anomalies over the Altiplano exceeding +1.5σ. The southerly cross-equatorial flow over South America has reached its maximum strength. The NASH southwestern boundary has visibly shifted equatorward (Figure 4) in response to the increase of geopotential which exceeds +1σ over the tropical and subtropical North Atlantic. The 850 hPa geopotential height has reached its maximum strength on Day 0.

On Day +1 (Figures 3g and 3h), cold anomalies continue to develop along the axis of the frontal system and temperatures of tropical South America north of the equator drop by over 1.5σ. Geopotential height anomalies at 850 hPa also exceed +1.5σ in the tropics, setting up anomalous temperature and geopotential gradients between northern hemisphere South America and the adjacent Intra-Americas Sea to the north. In response to the sustained geopotential height anomalies, the NASH boundary retains its equatorward expansion with the western ridge changing character from the "northern ridging type" to the "southern ridging type," as characterized by *Li et al.* [2011, 2013]. The geopotential anomalies along the NASH southern boundary still exceed +1σ. On Day +2 (Figures 3i and 3j), cold surface temperature anomalies weaken along the frontal system axis as the front extends into the tropics, but still remain below −1.5σ in parts of northern hemisphere South America (Figure 3i). Following the distribution of cold surface temperature anomalies, the center of the positive anomalies at 850 hPa shifts to the equatorial Amazon and over the tropical Atlantic Ocean. The strength of the positive geopotential anomalies begin to decay. The southerly cross-equatorial flow over Amazonia also weakens, and the NASH southern boundary retreats poleward, although not as far north as it is on Day −2.

Figure 4 shows that the NASH position falls within 1σ of the JJA averaged NASH position in the first 2 days before the cold surges arrive. However, during Days 0 and +1, the JJA NASH southern boundary expands beyond its range of 2σ from its mean position. In addition, the positive geopotential anomalies exceed +1σ over the southern part of the NASH. These changes together suggest significant change of the lower tropospheric circulation over the northern hemisphere Atlantic Ocean, including the southern part of the NASH. Also shown is a significant westward expansion of the NASH western boundary (Figure 4) before, during, and after these southern hemisphere cold surge events.

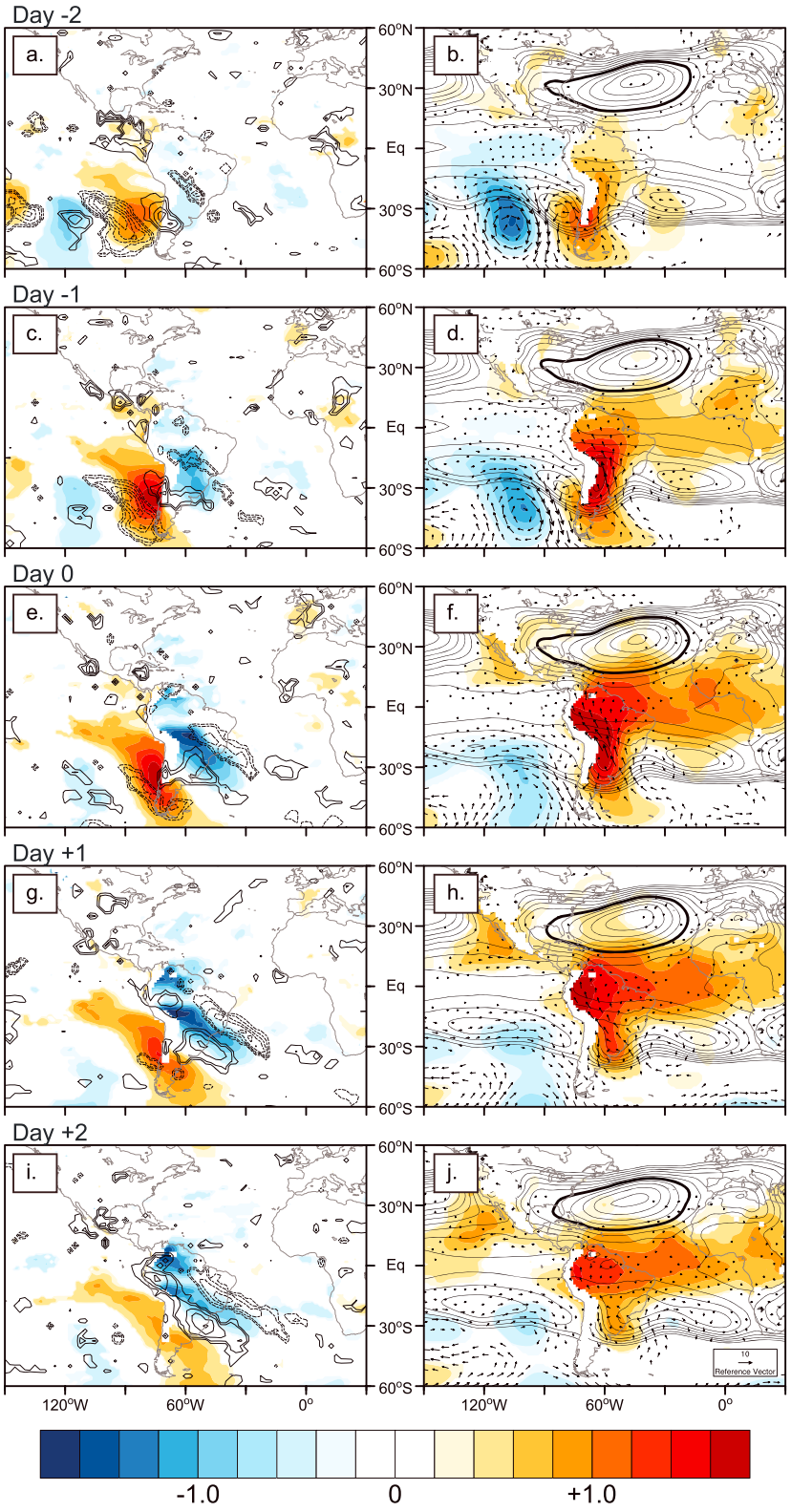

Figure 3. Daily lead-lag composite maps based on the cold surge events shown in Figure 2. (a, c, e, g, and i) Top of atmosphere OLR positive (solid contours) and negative (dashed contours) anomalies and standardized 850 hPa air temperature anomalies (shades). (b, d, f, h, and j) The 850 hPa geopotential height (contours) from 1500 to 1610 gpm with the NASH boundary (1560 gpm) bolded, 850 hPa horizontal wind anomalies (vectors), and standardized 850 hPa geopotential height anomalies (shades). Only anomalous values that are locally significant at 95% confidence are shown.

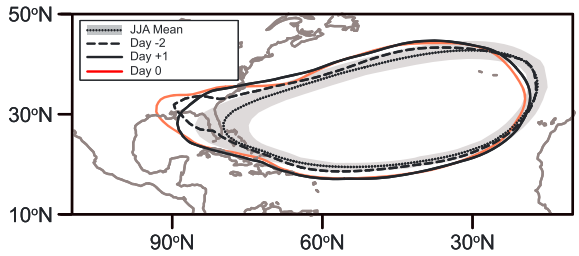

Figure 4. Overlay plot of the NASH boundary (1560 gpm at 850 hPa) for Day −2 (dashed black line), Day 0 (red line), Day +1 (solid black line), and the summer mean and standard deviation (dotted black line and gray shading). The Days −2, 0, and +1 contours are taken from Figure 3.

Figure 5 shows the anomalous upper tropospheric circulation associated with the cold surges, as represented by the composite anomalous 200 hPa horizontal wind and standardized geopotential height for the same events as in Figures 3 and 4. For brevity, we only show the composites for Days +2, 0, and +1. A Pacific-South American wave train emanating from the South Pacific can be seen (Figure 5a). Its cyclonic center begins to develop over extratropical South America on Day −2. Westerly wind anomalies also develop in the southern hemisphere tropical eastern Pacific, South America, and Atlantic Ocean from 20°S to the equator. On Day 0 (Figure 5b), the cyclonic anomalous center has moved into subtropical South America and the anticyclonic center to extratropical South America. Westerly anomalies in southern hemisphere Amazonia and adjacent oceans have intensified. The 200 hPa westerly wind anomalies shown in Figure 5 are larger in magnitude than their climatological easterlies, leading to episodes of westerly winds (total) at the equator in a climatologically easterly wind regime during June–August (Figure 1c). On Day +1 (Figure 5c), both the cyclonic and anticyclonic anomalous centers over South America begin to dissipate. However, there is virtually no significant upper tropospheric circulation anomaly in the northern hemisphere over the American-Atlantic sector before, during, and after the cold surges, due to the dominance of the upper tropospheric easterlies north of the equator. Thus, the observed lower tropospheric geopotential height and wind anomalies in Figure 3 cannot be explained by deep tropospheric circulation changes or cross-equatorial Rossby wave propagation.

Figure 6 investigates the vertical structure of the anomalous circulation associated with the deep equatorial incursions of the southern hemisphere cold surges; we show composites of vertical and meridional wind anomalies and standardized geopotential height anomalies in the meridional-height cross section of the troposphere ranging from 45°S to 45°N and averaged from 57.5°W to 62.5°W from 2 days before to 2 days after the cold surges. Only locally significant values are shown, and the geopotential height anomalies exceeding $+1\sigma$ are outlined by the dashed white contour. On Day −2 (Figure 6a), a southerly wind extending the depth of the troposphere is evident in the southern hemisphere subtropics and is indicative of a South American cold surge. The negative geopotential anomalies centered at 20°S at upper levels correspond to the midcontinental trough over South America (see Figure 5). Weak, positive low-level geopotential

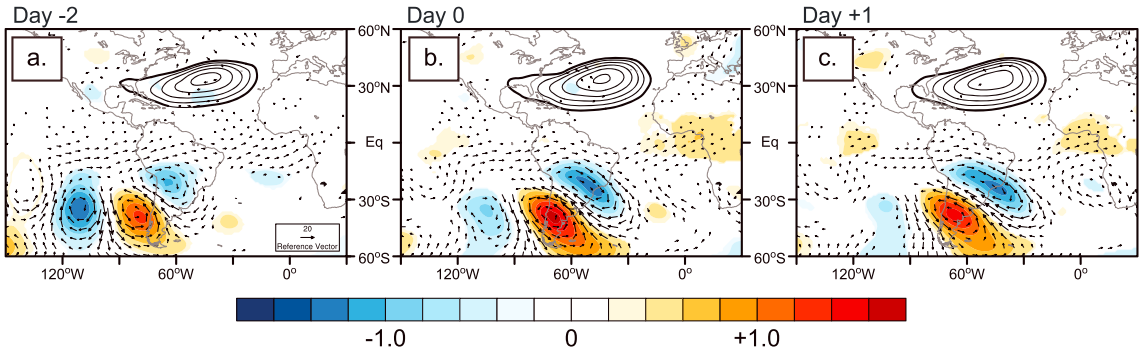

Figure 5. Daily lead-lag composite maps of the cold surge events for (a) Day −2, (b) Day 0, and (c) Day +1. Each panel displays 850 hPa geopotential height (contours) from 1560 to 1700 gpm with the NASH boundary (1560 gpm) bolded, 200 hPa horizontal wind anomalies (vectors), and standardized 200 hPa geopotential height anomalies (shading). Only anomalous values that are locally significant at 95% confidence are shown.

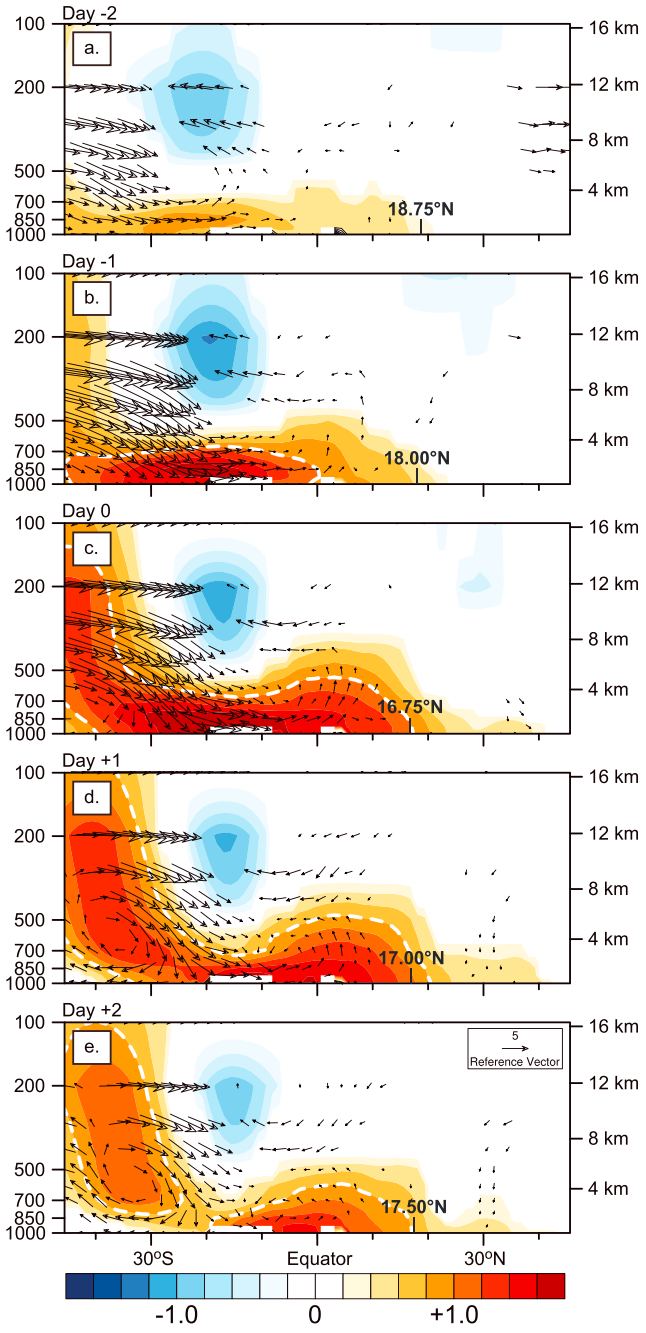

Figure 6. Daily lead-lag composites of the pressure-latitude cross section averaged from 62.5°W to 57.5°W based the cold surge events shown Figure 2. Fields displayed are standardized column geopotential height anomalies (shades) with the +1σ contour denoted by the white dashed line, and meridional and vertical wind anomalies (vectors). The lowest latitude of the NASH southern boundary (from Figure 2) is indicated for reference. Only locally significant values at 95% confidence are shown for each field.

anomalies are already developing across the South American continent and extending into the northern hemisphere as the cold surge begins. The southerly wind strengthens with the advancing cold surge on Day −1 (Figure 6b), and southern hemisphere geopotential height anomalies over South America begin to exceed +1σ in the lower troposphere from the midlatitudes to the tropics, due to cold temperature advection by the cold surges. Also, note that any wind or geopotential height anomalies present in the northern hemisphere are very weak. As the anomalous geopotential height gradient is increased in the tropical northern hemisphere, a hint of weak overturning can be seen in the circulation anomalies, with an upward branch at about 10°N and return flow to the southern hemisphere in the middle troposphere.

By Day 0 (Figure 6c), the cold surge advances into the deep tropics at low levels, and a tongue of increased geopotential height follows, with anomalies exceeding +1σ extending into the northern hemisphere subtropics. The strong subtropical geopotential height anomalies north of the equator occur with the equatorward migration of the NASH's southern boundary shown in Figures 3 and 4. Cooling over the northern hemisphere portion of South America and the strong meridional geopotential height gradient set up by the cold surge create conditions conducive to the development of a shallow meridional circulation in the lower and middle tropical troposphere, with low-level winds flowing northward and a southward return flow at about 5°N between 700 and 500 hPa, consistent with the anomalously low geopotential center in the middle and upper troposphere over the tropical southern hemisphere.

Figure 3h (Day +1) shows that the NASH remains equatorially extended and that its western boundary takes on a "southwest ridging" character [*Li et al.*, 2013]. These events happen as the anomalous shallow meridional circulation is strengthened at Day +1 (Figure 6d) with anomalous divergence occurring at 10°N–15°N in

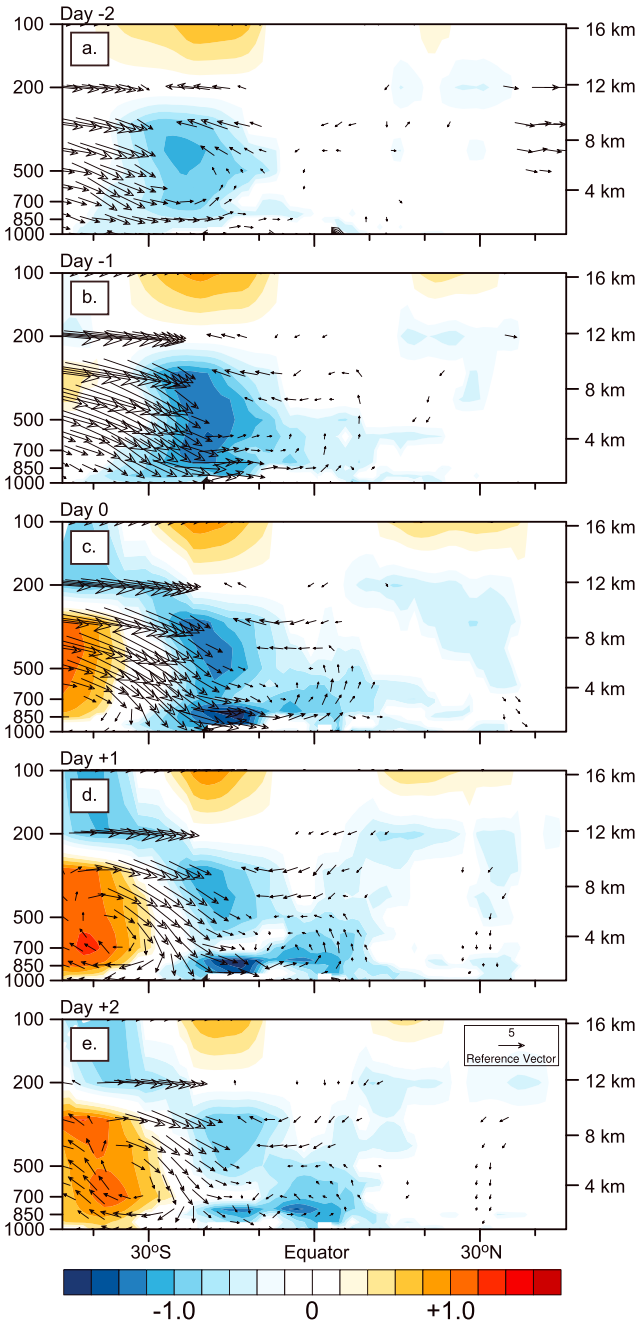

Figure 7. As in Figure 6 but for the standardized temperature anomalies (shades).

response to its overturning. The low-level tongue of $+1\sigma$ geopotential height anomalies remains deep in the northern hemisphere subtropics as the NASH expands equatorward, and anomalous subsidence can be detected in the NASH core region at 30°N, consistent with the colder lower tropospheric temperature in the northern hemisphere subtropics (Figures 3c, 3e, and 3g). On Day +2 (Figure 6e), the low-level geopotential anomalies and anomalous shallow meridional circulation weaken as the cold surge weakens. However, geopotential height anomalies greater than $+1\sigma$ can still be detected as far north as 11°N with significant anomalies of lower magnitude in the subtropics. The timing of the weakening of anomalous geopotential height on Day +2 occurs simultaneously with the first signs of contraction of the NASH southern boundary (Figure 3j).

Figure 7 shows the composite air temperature anomalies superimposed with meridional and vertical winds from 2 days before to 2 days after the cold surges. Cold temperature anomalies in the deep tropospheric column (surface to 300 hPa) are apparent from Day −2 to Day +2 between 40°S and 5°S, indicating a deep equatorward penetration of the cold fronts peaking at Days −1 and 0. The standardized cold temperature anomalies at the center of these cold surges are close to 2, indicating that these events represent extreme cold surges, close to 99 percentile. From 5°S to as far north as 20°N, cold temperature anomalies are evident below 500 hPa from Days −1 to +2, indicating a northward cold air advection by the shallow cross-equatorial circulation. The return flow occurs first above the middle troposphere (500–300 hPa) during Days −1 to 0, then in the lower to middle troposphere (700–500 hPa) during Days +1 and +2 are evident. The temperatures of the return flow are close to their climatological values, presumably because temperature changes in the equatorial area are generally small except when deep cold surges occur.

The evolution of the southerly cross-equatorial flow in the lower tropospheric as represented by the V index, the strength of shallow boundary/returning flow, the lower tropospheric (850 hPa) geopotential height gradient, and the lower tropospheric zonal wind along the southern edge of the NASH associated with the cold surges is explored through the composite time series of these variables from 5 days before to 5 days

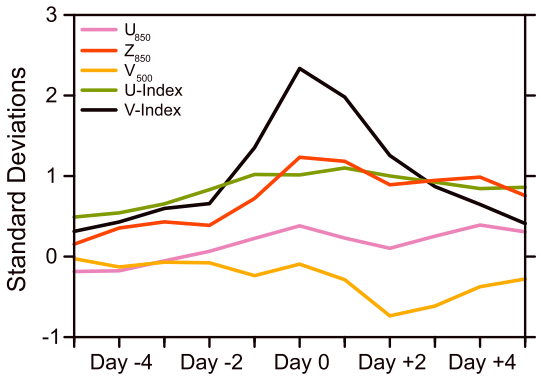

Figure 8. Composite time series for various standardized fields from 5 days before to 5 days after composite conditions are met. U_{850} represents the domain average zonal wind at 850 hPa from 12.5°N to 17.5°N and 60°W to 50°W along the southern NASH boundary in the western Atlantic Ocean. Z_{850} represents the domain average geopotential height at 850 hPa along the lowest extent of the southern NASH boundary from 10°N to 15°N and 60°W to 40°W. V_{500} represents the shallow circulation return flow at 500 hPa from −5°S to −5°N and 75°W to 65°W. U index and V index represent the 200 hPa zonal and 925 hPa meridional wind as defined in the composite conditions.

after the cold surges in Figure 8. The strength of the shallow circulation return flow is indicated by the area averaged 500 hPa meridional wind between 5°S and 5°N, 65°W and 75°W. The 850 hPa geopotential height averaged over the area where NASH's southwestern boundary is generally located is used to indicate the influence of the cold surges on the southwestern portion of the NASH. Figure 8 shows that the 200 hPa westerly wind anomalies (U index) of 1σ persist from Days −5 to +5. The V index increases rapidly from Days −2 to 0 reaching more than 2σ. This increase suggests a strong and rapidly increasing cross-equatorial northward cold advection in the lower troposphere and follows the cooling of temperature associated with cold surges that peak at Day −1 (see Figures 7a–7c). The 850 h Pa geopotential height at the southwestern edge of the NASH peaks by Day 0 and remains high until at least Day +5. The southward return flow in the midtroposphere (V_{500}) does not become evident until after Day 0. It peaks on Day +2 and dissipates on Day +5. The timing of the midtropospheric return flow strongly suggests that it is a part of a shallow cross-equatorial circulation induced by the cold surges, instead of a direct deep direct thermal circulation (or regional manifestation of the Hadley circulation). The zonal wind anomalies at 850 hPa along southern edge of the NASH are less than 0.5σ and thus insignificant.

The analyses shown in Figures 6–8 suggest that the strong increase of southerly low-level cross-equatorial flow over South America, the increase of 850 hPa geopotential height over the tropical and subtropical North Atlantic, and the resulting southward expansion (and perhaps strengthening) of the NASH are linked by the anomalous shallow meridional circulation induced by deep equatorward incursions of the cold surges from extratropical South America.

4. Discussion

The results shown in the previous section raise several questions: Could a deep monsoonal circulation be responsible for the episodes of extreme southerly cross-equatorial flow in the lower troposphere and anomalous shallow meridional circulation? What causes the absence of cross-equatorial upper tropospheric circulation response to the cold surges? What drives such a far reaching anomalous shallow cross-equatorial circulation? What are the major uncertainties of this study? We briefly discuss potential answers to these questions in this section.

The deep tropospheric monsoonal circulation driven by deep convection over North America and Atlantic Intertropical Convergence Zone can also increase southerly cross-equatorial flow over South America and Atlantic [e.g., *Trenberth et al.*, 2000; *Wang and Fu*, 2002; *Wang et al.*, 2011; *Fu et al.*, 2016]. However, the extreme southerly cross-equatorial flow (>2σ) does not occur until Day 0 (Figure 8), 1 day after the extreme cold surges reach their north-most latitudes (5°S, Day −1; Figure 7b). Figures 6c–6e and 7c–7e show that such extreme southern cross-equatorial flow is associated with the anomalous shallow meridional circulation, and upper tropospheric circulation anomalies over the equatorial and northern hemisphere tropical region are absent. We do not know whether an anomalous deep tropospheric monsoonal circulation, driven by northern hemisphere deep convection, can also induce extreme southerly cross-equatorial flow in the lower troposphere, or what are the relative influences of the shallow and deep circulation on the cross-equatorial flow over South America, questions appropriate for future study.

Why is there no cross-equatorial upper tropospheric circulation response to the cold surges? The upper tropospheric westerly anomalies are confined in the southern hemisphere (Figure 5). The northern hemisphere upper troposphere is still dominated by easterlies, preventing cross-equatorial propagation of the Rossby waves. In addition, boreal summer is the dry season over southern Amazonia. That relatively dry and stable atmosphere tends to suppress large-scale increase of deep convection in that region, despite the frequent incursions of strong cold surges. This suppression apparently prevents generation of convective coupled Kelvin waves in the equatorial South America and Atlantic. These conditions probably are responsible for lack of a cross-tropospheric influence in the upper troposphere.

Shallow meridional cross-equatorial circulation, driven by a strong sea surface temperature gradient, has been found to be a mechanism for interhemisphere connection over the tropical eastern oceans [*Zhang et al.*, 2008]. Although the shallow cross-equatorial circulation in our study is driven by cross-equatorial cold air advection induced by extreme cold surges from extratropical South America, the dynamic mechanism is similar to that driving the shallow meridional cross-equatorial circulation over the tropical eastern oceans [*Nolan et al.*, 2007]. However, these cold-surge-driven shallow cross-equatorial circulations extend over a much broader latitudinal range from the southern hemisphere subtropical South America (~35°S; Figures 5c and 5d) to the northern hemisphere tropical and subtropical Atlantic Ocean (18°N). The cause of such far-reaching shallow cross-equatorial circulation is not clear, but the configuration of the South American continent, especially its topographic forced flow on the eastside of the Andes and lee genesis [e.g., *Gan and Rao*, 1994; *Garreaud and Wallace*, 1998] and extension of the large landmass and Andes to 10°N, may enable unusually deep equatorward penetration of well preserved cold surges over South America (Figures 3e, 3g, 3l, and 7b–7d). The resultant strong cooling of the lower troposphere that extends to 10°N (Figures 7d–7d) is likely in part responsible for the extension of the shallow anomalous cross-equatorial circulation to subtropical North Atlantic.

This work is mainly based on an atmospheric reanalysis product. Although such products provide the most realistic available description of atmospheric state and variability, they can have considerable uncertainty [*Ling and Zhang*, 2013]. For example, all of the reanalysis products show a shallower peak of atmospheric diabatic heating over the South American sector than that derived from atmospheric soundings [*Ling and Zhang*, 2013]. Although deep convection is infrequent over southern Amazonia during boreal summer, such a bias still could lead to an underestimate of the depth of the circulation response to convective heating over tropical South America that is shown in Figure 6. Future work on this topic should include a reproduction of these results across various reanalysis data sets other than MERRA. It is also important to determine if weather and climate models realistically produce the observed cross-equatorial influence from South American cold surges, and how more realistic representations of these processes could contribute to more accurate weather forecasting and future climate projections over the North Atlantic Ocean.

While the composite lower tropospheric wind anomalies over the south and western NASH region associated with these cold surges appear to be insignificant (Figures 3f–3j), strong wind anomalies during individual cold surges events are apparent (not shown). Thus, whether cold surges have a significant impact on lower tropospheric winds along the NASH's south and western edges, especially the Caribbean jet and Gulf inflow to southeastern or south-central U.S. need further investigation.

5. Conclusions

The influences of cold surges from one hemisphere on tropical weather and circulation of the opposite hemisphere during boreal winter (December–February), when the upper tropospheric westerly prevails in the equatorial region, have been reported extensively in literature. Such cross-equatorial teleconnection is generally not expected during boreal summer (June–August) when the upper tropospheric easterly prevails in the equatorial region. We have observed that deep equatorward penetrations of extreme cold surges originating from extratropical South America during boreal summer (austral winter) can reduce temperature and increase lower tropospheric pressure over the tropical and subtropical North Atlantic, strengthening and expanding the southwestern part of the NASH equatorward. Such an influence is carried out by an anomalous shallow meridional circulation across the equator.

These events occur when episodes of extreme cold surges and upper tropospheric (200 hPa) westerlies occur simultaneously over the southern and equatorial Amazonia. Upper tropospheric westerly allow for

equatorward propagation of the Rossby waves and associated strong cold surges from extratropical South America deep into the southern Amazon reaching to 5°S. However, an upper tropospheric large-scale circulation response in the northern hemisphere to these southern hemisphere cold surges is absent, presumably due to the relatively dry and stable atmosphere over southern hemisphere Amazonia and prevailing upper tropospheric easterlies in the equatorial and tropical northern hemisphere South America-Atlantic sector.

In the lower troposphere, strong northward advection of the cold and dense air continues deep into the northern hemisphere tropics and subtropics in the Atlantic-American sector. The resultant cooling increases pressures in the lower troposphere over the tropical and subtropical North Atlantic up to 18°N. The latter projects onto the southern edge of the NASH, increasing its pressure and leading to equatorward expansion of its southern boundary. The strong cooling of the lower troposphere from southern Amazonia to the tropical North Atlantic also enhances the northward pressure gradient in the lower to middle troposphere from the southern Amazonia to subtropical North Atlantic, consistent with the anomalous shallow northerly return flow across the equator. This shallow northerly return flow and the southerly cross-equatorial flow in the lower troposphere (below 700 hPa) together form a strong anomalous shallow cross-equatorial circulation. It is this shallow anomalous circulation that enables the extreme cold surges from extratropical South America to influence lower tropospheric temperature and pressure fields over the tropical to subtropical North Atlantic, including equatorward expansion of the NASH's southern edge.

During boreal summer, surface temperature and circulation over the tropical and subtropical Atlantic, and the southern edge of the NASH play important roles in determining moisture transport to North America and hurricanes or tropical storm tracks. However, we do not have a clear predictive understanding of the processes that control their variabilities. Most of the previous studies have been focused [*Wang and Fu*, 2007] on the influences from northern hemisphere and the tropical Atlantic ocean. This study shows that extreme cold surges from extratropical South America can also influence surface temperature and circulation over the tropical and subtropical Atlantic and the southern edge of the NASH. These extreme cold surges can be clearly monitored and tracked at lease several days back in time before they reach tropical southern Amazonia and influence tropical and subtropical North Atlantic [e.g., *Garreaud and Wallace*, 1998]. Thus, they can provide a potential source of predictability for lower tropospheric circulation anomalies, including NASH's southern edge, during boreal summer. Further studies on the conditions that control the impacts of these extreme cold surges on North Atlantic and southeast and south-central United States during the individual cold surge events are needed in order to more clearly understand their impacts at weather time scale (days to 1 week) and determine their value for improving predictability of the weather patterns, including the tropical storms, over the tropical and subtropical Atlantic and potentially southeastern and south-central United States.

Acknowledgments

We thank John Michael Wallace for his encouragement and insightful comments that have reshaped the focus of this study and substantially improved our analysis. This work is supported by the National Science Foundation (AGS 0937400), the National Oceanic and Atmospheric Administration Modeling, Analysis, Predictions, and Projections Program (NA10OAR4310157), and Jackson School of Geosciences, The University of Texas at Austin. P.A. Arias is supported by Colciencias grant 115-660-44588. The two data sets used in this work are publically available: MERRA 3 h reanalysis product is available at http://disc.sci.gsfc.nasa.gov/datasets/MAI3CPASM_V5.2.0/summary?keywords=merra. NOAA Interpolated Outgoing Longwave Radiation (OLR) is available at http://www.esrl.noaa.gov/psd/data/gridded/data.interp_OLR.html. All data for this paper are properly cited and referred to in the reference list.

References

Arias, P. A., R. Fu, and K. C. Mo (2012), Decadal variation of rainfall seasonality in the North American monsoon region and its potential causes, *J. Clim.*, *25*(12), 4258–4274.

Arias, P. A., R. Fu, C. Vera, and M. Rojas (2015), A correlated shortening of the North and South American monsoon seasons in the past few decades, *Clim. Dyn.*, *45*(11–12), 3183–3203.

Charney, J. G. (1963), A note on large-scale motions in the tropics, *J. Atmos. Sci.*, *20*(6), 607–609, doi:10.1175/1520-0469(1963)020<0607:Anolsm>2.0.Co;2.

Charney, J. G. (1969), A further note on large-scale motions in tropics, *J. Atmos. Sci.*, *26*(1), 182–185, doi:10.1175/1520-0469(1969)026<0182:Afnols>2.0.Co;2.

Chen, P., M. P. Hoerling, and R. M. Dole (2001), The origin of the subtropical anticyclones, *J. Atmos. Sci.*, *58*(13), 1827–1835.

Dickinson, R. E. (1970), Development of a Rossby wave critical level, *J. Atmos. Sci.*, *27*(4), 627–633, doi:10.1175/1520-0469(1970)027<0627:Doarwc>2.0.Co;2.

Davis, R. E., B. P. Hayden, D. A. Gay, W. L. Phillips, and G. V. Jones (1997), The north atlantic subtropical anticyclone, *J. Clim.*, *10*(4), 728–744.

Diem, J. E. (2006), Synoptic-scale controls of summer precipitation in the southeastern United States, *J. Clim.*, *19*(4), 613–621, doi:10.1175/jcli3645.1.

Fu, R., P. A. Arias, and H. Wang (2016), The connection between the North and South American Monsoons, in *The Monsoons and Climate Change*, edited by L. de Carvalho and C. Jones, pp. 187–206, Springer, Cham.

Gan, M. A., and V. B. Rao (1994), The influence of the Andes Cordillera on transient disturbances, *Mon. Weather Rev.*, *122*(6), 1141–1157, doi:10.1175/1520-0493(1994)122<1141:tiotac>2.0.co;2.

Garreaud, R. D. (2000), Cold air incursions over subtropical South America: Mean structure and dynamics, *Mon. Weather Rev.*, *128*(7), 2544–2559.

Garreaud, R. D., and J. M. Wallace (1998), Summertime incursions of midlatitude air into subtropical and tropical South America, *Mon. Weather Rev.*, *126*(10), 2713–2733.

Henderson, K. G., and A. J. Vega (1996), Regional precipitation variability in the southern United States, *Phys. Geogr.*, *17*(2), 93–112.
Hoskins, B. J., and G.-Y. Yang (2000), The equatorial response to higher-latitude forcing, *J. Atmos. Sci.*, *57*(9), 1197–1213.
Lau, K.-M., and M.-T. Li (1984), The monsoon of East Asia and its global associations—A survey, *Bull. Am. Meteorol. Soc.*, *65*(2), 114–125.
Kelly, P., and B. Mapes (2011), Zonal mean wind, the Indian monsoon, and July drying in the western Atlantic subtropics, *J. Geophys. Res.*, *116*, D00Q07, doi:10.1029/2010JD015405.
Li, L., R. Li, Y. D. Fu, and H. Wang (2011), Changes to the North Atlantic subtropical high and its role in the intensification of summer rainfall variability in the southeastern United States, *J. Clim.*, *24*(5), 1499–1506.
Li, L., W. Li, and Y. Kushnir (2012), Variation of the North Atlantic subtropical high western ridge and its implication to southeastern US summer precipitation, *Clim. Dyn.*, *39*(6), 1401–1412.
Li, L., R. Li, Y. D. Fu, and H. Wang (2013), Reply to "Comments on 'Changes to the north Atlantic subtropical high and its role in the intensification of summer rainfall variability in the southeastern United States'", *J. Clim.*, *26*(2), 683–688.
Li, W., and R. Fu (2006), Influence of cold air intrusions on the wet season onset over Amazonia, *J. Clim.*, *19*(2), 257–275.
Liebmann, B. (1996), Description of a complete (interpolated) outgoing longwave radiation dataset, *Bull. Am. Meteorol. Soc.*, *77*, 1275–1277.
Liebmann, B., G. N. Kiladis, L. M. Carvalho, C. Jones, C. S. Vera, I. Bladé, and D. Allured (2009), Origin of convectively coupled kelvin waves over South America, *J. Clim.*, *22*(2), 300–315.
Ling, J., and C. Zhang (2013), Diabatic heating profiles in recent global reanalyses, *J. Clim.*, *26*(10), 3307–3325.
Liu, Y., G. Wu, and R. Ren (2004), Relationship between the subtropical anticyclone and diabatic heating, *J. Clim.*, *17*(4), 682–698.
Love, G. (1985a), Cross-equatorial influence of winter hemisphere subtropical cold surges, *Mon. Weather Rev.*, *113*(9), 1487–1498.
Love, G. (1985b), Cross-equatorial interactions during tropical cyclogenesis, *Mon. Weather Rev.*, *113*(9), 1499–1509.
Lupo, A. R., J. J. Nocera, L. F. Bosart, E. G. Hoffman, and D. J. Knight (2001), South American cold surges: Types, composites, and case studies, *Mon. Weather Rev.*, *129*(5), 1021–1041.
Marengo, J., A. Cornejo, P. Satyamurty, C. Nobre, and W. Sea (1997), Cold surges in tropical and extratropical South America: The strong event in June 1994, *Mon. Weather Rev.*, *125*(11), 2759–2786.
Miyasaka, T., and H. Nakamura (2005), Structure and formation mechanisms of the Northern Hemisphere summertime subtropical highs, *J. Clim.*, *18*(23), 5046–5065.
Nolan, D. S., C. Zhang, and S.-h. Chen (2007), Dynamics of the shallow meridional circulation around intertropical convergence zones, *J. Atmos. Sci.*, *64*(7), 2262–2285.
Parmenter, F. C. (1976), A Southern Hemisphere cold front passage at the equator, *Bull. Am. Meteorol. Soc.*, *57*(12), 1435–1440.
Pezza, A. B., and T. Ambrizzi (2005), Dynamical conditions and synoptic tracks associated with different types of cold surge over tropical South America, *Int. J. Climatol.*, *25*(2), 215–241.
Rienecker, M., J. Suarez, R. Gelaro, R. Todling, J. Bacmeister, E. Liu, M. G. Bosilovich, S. D. Schubert, L. Takacs, and G.-K. Kim (2011), MERRA: NASA's modern-era retrospective analysis for research and applications, *J. Clim.*, *24*(14), 3624–3648.
Radok, U., and A. M. Grant (1957), Variations in the high tropospheric mean flow over Australia and New Zealand, *J. Meteorol.*, *14*(2), 141–149.
Rodwell, M. J., and B. J. Hoskins (2001), Subtropical anticyclones and summer monsoons, *J. Clim.*, *14*(15), 3192–3211.
Seager, R., R. Murtugudde, N. Naik, A. Clement, N. Gordon, and J. Miller (2003), Air–sea interaction and the seasonal cycle of the subtropical anticyclones, *J. Clim.*, *16*(12), 1948–1966.
Straub, K. H., and G. N. Kiladis (2002), Observations of a convectively coupled kelvin wave in the eastern Pacific ITCZ, *J. Atmos. Sci.*, *59*(1), 30–53.
Tomas, R. A., and P. J. Webster (1994), Horizontal and vertical structure of cross-equatorial wave propagation, *J. Atmos. Sci.*, *51*(11), 1417–1430.
Trenberth, K. E., D. P. Stepaniak, and J. M. Caron (2000), The global monsoon as seen through the divergent atmospheric circulation, *J. Clim.*, *13*(22), 3969–3993.
Vera, C. S., and P. K. Vigliarolo (2000), A diagnostic study of cold-air outbreaks over South America, *Mon. Weather Rev.*, *128*(1), 3–24.
Wang, B., Q. Ding, and J. Liu (2011), Concept of global monsoon, in *The Global Monsoon System: Research and Forecast*, 2nd ed., pp. 3–14, World Sci., Singapore.
Wang, C., and S. K. Lee (2007), Atlantic warm pool, Caribbean low-level jet, and their potential impact on Atlantic hurricanes, *Geophys. Res. Lett.*, *34*, L02703, doi:10.1029/2006GL028579.
Wang, H., and R. Fu (2002), Cross-equatorial flow and seasonal cycle of precipitation over South America, *J. Clim.*, *15*(13), 1591–1608.
Wang, H., and R. Fu (2007), The influence of Amazon rainfall on the Atlantic ITCZ through convectively coupled kelvin waves, *J. Clim.*, *20*(7), 1188–1201.
Webster, P. J., and J. R. Holton (1982), Cross-equatorial response to middle-latitude forcing in a zonally varying basic state, *J. Atmos. Sci.*, *39*(4), 722–733.
Wilks, D. S. (2006), On "field significance" and the false discovery rate, *J. Appl. Meteorol. Climatol.*, *45*(9), 1181–1189.
Yu, L., and M. M. Rienecker (1998), Evidence of an extratropical atmospheric influence during the onset of the 1997–98 El Niño, *Geophys. Res. Lett.*, *25*(18), 3537–3540, doi:10.1029/98GL02628.
Zhang, C., D. S. Nolan, C. D. Thorncroft, and H. Nguyen (2008), Shallow meridional circulations in the tropical atmosphere, *J. Clim.*, *21*(14), 3453–3470.